In plane Shear Strength of Cross Laminated Timber (CLT): Test Configuration, Quantification and influencing Parameters

R BRANDNER [1) 2)]; T BOGENSPERGER [2)]; G SCHICKHOFER [1)]

Graz University of Technology, Institute of Timber Engineering and Wood Technology [1)]

Competence Centre holz.bau forschungs gmbh [2)]

1 Abstract

Cross laminated timber (CLT) has become a well-known and widely applied two-dimensional, engineered timber product worldwide. It constitutes a rigid composite of an odd number of orthogonal and glued layers. Focusing on a single glued node loaded in plane in shear and composed of two crossed board segments and the adhesive layer in-between, in principle three types of shear mechanisms can be distinguished: mechanism I "net-shear" (shearing perpendicular to grain), mechanism II "torsion" and mechanism III "gross-shear" (shearing parallel to grain). In fact, while having generally accepted values for the resistance against mechanism II and good estimates for mechanism III the resistance against "net-shear" (mechanism I) is still in discussion. In spite of numerous investigations on nodes and on whole CLT elements in the past, a common sense concerning the test procedure, the consideration and handling of distinct influencing parameters and the quantification of the shear strength are open.

We focus on the in plane shear resistance of single nodes according to mechanism I. We (i) propose a test configuration for reliable determination of the shear strength, (ii) determine the shear resistance in case of shear loads perpendicular to grain, (iii) discuss influences of some parameters on the shear strength of single nodes, and (iv) give a brief outlook concerning the resistance of CLT elements against shear loads in plane.

2 Introduction

Cross laminated timber (CLT) constitutes a solid, laminar engineered timber product with high resistances against loads in and out of plane. Common CLT is a rigid composite of an odd number of orthogonal and face bonded layers. Each single layer consists of side-by-side aligned (finger jointed) boards with or without edge bonding. In CLT without edge bonding gaps between the boards, more or less regular in width, are evident. Common gap widths allowed by technical approvals for CLT are 2 (3) mm in the top and 4 (6) mm in the core layers (Brandner 2013).

We focus on the mechanical properties of CLT loaded in plane. In particular, the resistance in plane in shear of CLT made of Norway spruce (*Picea abies*) is addressed. Three principle shear mechanisms are distinguished: mechanism I "net-shear", mechanism II "torsion" and mechanism III "gross-shear" (see e.g. Bogensperger et al. 2007 & 2010, Blaß and Flaig 2012). Mechanism I "net-shear" corresponds to shearing perpendicular to grain of the net cross sections in the controlling plane. Mechanism III "gross-shear" is associated with shearing parallel to grain of the whole CLT element. For clarification of these mechanisms, at first some simplifications for the mechanical treatment are made according to Bogensperger et al. (2010).

2.1 Some general Comments on the Shear Mechanisms

Following Bogensperger et al. (2010) a representative volume element (RVE) is introduced, which is in thickness equal to a CLT element and in width and depth equal to the width of one board plus the half of the width of gaps between adjacent boards. Focusing on shear in a CLT element with constant

layer thicknesses ($t_{l,i} \equiv t_l$, $i = 1, \ldots, N$) and an infinite number of layers $N \rightarrow \infty$ (neglecting boundary conditions) the RVE can be further simplified to a representative volume sub-element (RVSE). This RVSE is in width and depth equal to the RVE but in thickness equal to t_l, composed of both half thicknesses of two orthogonal boards in one node and the face bonding in-between (see Fig. 1).

As consequence of $N \rightarrow \infty$ a proportional shear force $n_{xy,\mathrm{RVSE}}$ instead of the overall shear force n_{xy} is defined. The nominal shear stress τ_0 is given as (see Bogensperger et al. 2010)

$$\tau_0 = \frac{n_{xy,\mathrm{RVSE}}}{a \cdot t_l}, \tag{1}$$

with a as width and depth, and t_l as thickness of the RVSE, respectively. This more theoretical shear stress corresponds to **mechanism III** "gross-shear" (see Fig. 1). Thereby a constant shear stress distribution over the cross section is assumed, which may lead to shear failures parallel to grain in all layers. Therefore, an intact edge bonding between the boards within one layer and the absence of checks is required. Missing or insufficient connection between the boards at the edges disables the transfer of shear stresses in that direction. For the resistance against mechanism III Blaß and Flaig (2012) recommend a characteristic (5 %-quantile) shear strength of $f_{v,\mathrm{gross,k}} = 3.5$ N/mm². In view of EN 338 and with $k_{\mathrm{cr}} = 1.00$ (factor which considers the influence of cracks on the shear strength) a value of $f_{v,\mathrm{gross,k}} = 4.0$ N/mm² for CLT composed of boards of strength class C24 according to EN 338 (the common material used for CLT in Europe) is proposed (Flaig and Blaß 2013). In case of stress relieves adaptation of $f_{v,\mathrm{gross}}$ seems to be necessary.

Of course, in CLT composed of layers without edge bonding, shear force can only be transferred via the cross sections of boards and via the gluing interface of the face bonding. Comparable conditions are expected in edge bonded CLT exposed to common climate variations. Moisture induced stresses caused by these climate variations lead to checks, which again restrict the possibilities for shear transfer. Consequently, mechanism I and II become active and their verification mandatory in the design process, even in cases of gap widths $t_{\mathrm{gap}} \rightarrow 0$.

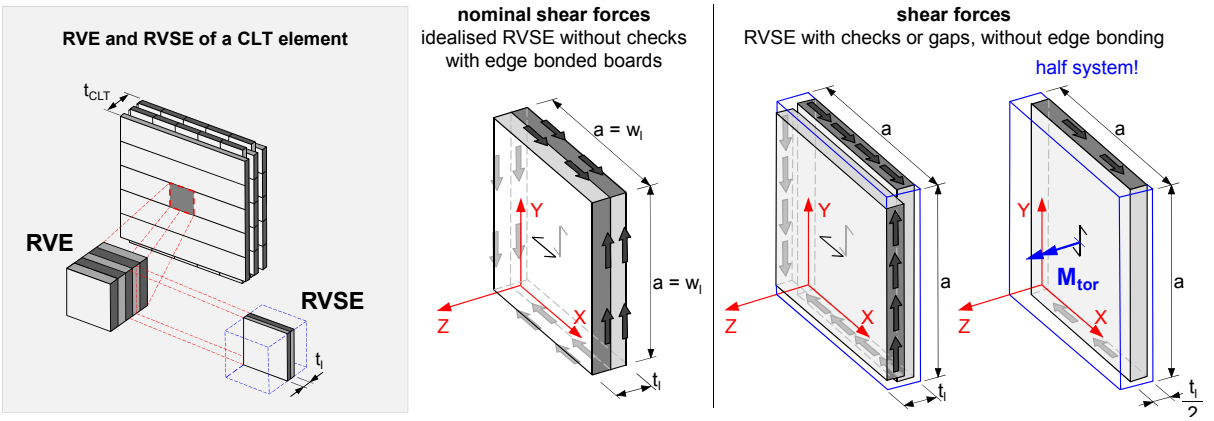

Fig. 1: (block left) RVE and RVSE of a CLT element; (block right) shear stresses in a RVSE: nominal shear stress τ_0 (left), real shear stress τ_{net} (middle; superposing left & right), torsional stress τ_{tor} on the gluing interface (right) (Bogensperger et al. 2010; adapted)

Mechanism I considers the transfer of shear forces via the cross sections of boards within a RVSE. Consequently, the shear stress is given as

$$\tau_{\mathrm{net}} = 2 \cdot \tau_0, \tag{2}$$

with τ_{net} as the shear stress dedicated to the net cross section (see Fig. 1). For calculation of stresses caused by n_{xy} in a real CLT element, considering e.g. boundary conditions caused by finite N and variations in layer thickness, a procedure is provided e.g. in Bogensperger et al. (2010).

Shear strain in the RVSE, in case of insufficient or missing connection between the board edges, causes also torsional strain in the surface bond layer. This may cause failure in the gluing interface, which is dedicated to **mechanism II** "torsion" (see Fig. 1). Assuming polar torsion, the torsional shear stresses τ_{tor} are given as

$$\tau_{tor} = \frac{M_{tor}}{I_p} \cdot \frac{a}{2} = 3 \cdot \tau_0 \cdot \frac{t_l}{a}, \quad (3)$$

with M_{tor} as torsional moment and I_p as polar moment of inertia. Consequently, τ_{tor} depends on the geometric parameter ratio t_l / a. Thus, in a real CLT element with varying layer thicknesses the thickest layer governs the design (Bogensperger et al. 2010). Concerning the resistance of a RVSE against torsion, numerous investigations were made in the past, e.g. Blaß and Görlacher (2002), Jeitler (2004) and Jöbstl et al. (2004). A possible redistribution of torsional stresses from zones exposed to rolling shear to zones exposed to shear is mentioned. Despite some influences of parameters (i) annual ring pattern, and (ii) surface area under torsion (see e.g. Jeitler 2004, Jöbstl et al. 2004) there is common sense to use $f_{tor,k}$ = 2.5 N/mm² as characteristic (5 %-quantile) torsional shear strength.

To conclude, in a real CLT element at common use the occurrence of checks due to climate variations or gaps due to missing edge bonding, in the design process both shear mechanisms, mechanism I "net-shear" and mechanism II "torsion", need verification. As there is common sense on the resistance against torsion in the gluing interface this contribution concentrates on the determination and quantification of the resistance against shear according to mechanism I.

2.2 Shear Mechanism I "net-shear": State-of-the-Art

In general, investigations on the shear strength of CLT in plane by testing can be classified in (i) investigations performed on whole CLT elements (e.g. Bosl 2002, Bogensperger et al. 2007, Andreolli et al. 2012), and (ii) investigations performed on single nodes (in dimension corresponding to a double or multiple RVSE; e.g. Wallner 2004, Jöbstl et al. 2008, Hirschmann 2011).

2.2.1 Investigations on CLT Elements

Bosl (2002) report on tests conducted on five-layer CLT elements with dimension 1,200 x 1,200 x 85 (5 x 17 mm) mm³. The elements were freely placed in a squared, diagonally in tension loaded four-hinged steel-frame (see Fig. 2, left). Consequently, the CLT was stressed in shear and compression. In all four specimens with orthogonal layers, the ultimate load was limited by buckling of single boards in the top-layers as consequence of delaminated layers. An insufficient surface bonding can be concluded. A significant damage of the elements at zones of load introduction was not observed. The mean ultimate load was $F_{max,mean}$ = 325 kN, which corresponds to shear stresses of $\tau_{gross,mean} \equiv \tau_{0,mean} \approx 2.3$ N/mm² and $\tau_{net,mean} \approx 5.6$ N/mm².

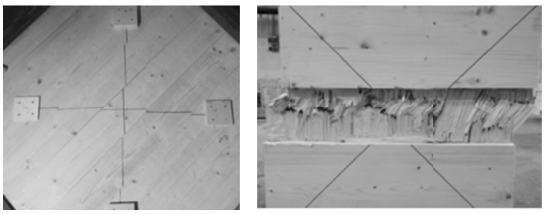

Fig. 2: Tests on CLT elements: Bosl (2002; left), Andreolli et al. (2012; right)

Later, Traetta et al. (2006) and Bogensperger et al. (2007) made tests on three-layer CLT elements of dimension 560 x 560 x 120 (30 + 60 + 30 mm) mm³, with gaps between the boards of 5 mm. A steel frame with two squared test fields, equal in size and hinged at all corners, was used for the three-point bending tests. The load on the steel frame was applied in compression. For a continuous load transfer the CLT elements were continuously bonded to the steel frame and at the boarders reinforced by hardwood lamellas (see Fig. 3, left). However, the observed failures were not in shear but locally in compression. Nevertheless, considering the inner shear field of 5 x 5 boards per layer and all five tests a maximum shear stress of at least $\tau_{net,mean} \approx 6.0$ N/mm² (F_{max} = 78.1 to 134.0 kN) can be calculated.

Andreolli et al. (2012) mention tests on three and five layer CLT elements loaded (i) edgewise in four-point bending as well as (ii) diagonally in compression by means of short steel angles. In test group (ii) two of four tests failed in torsion (one with edge bonding but cracks, the other without edge bonding), one delaminated in the lateral surfaces (three layer specimen with edge bonding), and the forth failed in shear perpendicular to grain, allocable to mechanism I (Fig. 2, right). This last test provided $f_{v,net}$ = 12.7 N/mm² as maximum value of shear stress. The stress calculation was carried out dividing the maximum load by the net cross section multiplied by a correction factor, taking into account the real stress distribution in diagonal compression test, which is not pure shear stress but an

interaction between shear and compression in the central area of the panel (Andreolli et al. 2012). A test procedure for CLT columns with nodes stressed in 45° angle can also be found in Kreuzinger and Sieder (2013). Although a successful verification of the proposed procedure by tests is mentioned, the data is not presented.

CUAP (2005) provides a test configuration for determination of shear strength for European Technical Approvals (ETAs) based on the four-point bending test according to EN 408. A gap between the longitudinal boards enforces transfer of shear forces via the cross layers and the gluing interfaces. However, Jöbstl et al. (2008) and other report that in almost all cases not the intended failure in shear perpendicular to grain according to mechanism I, but rather bending failures occur. Jöbstl et al. (2008) mention eight test series of three and five layer CLT elements (in total 90 specimens) tested according to the CUAP procedure. None of these specimens failed in shear perpendicular to grain; nearly 100 % failed in bending between the loading points. Some exceptions failed in rolling shear or in shear parallel to grain, whereby both failure mechanisms are not conform to the failure scheduled for shear verification. According to CUAP this has to be done on the net cross section. The observed mean shear stresses $\tau_{net,mean}$ at bending failure are in the range of 5.4 to 11.5 N/mm², with an overall weighted mean of 8.4 N/mm².

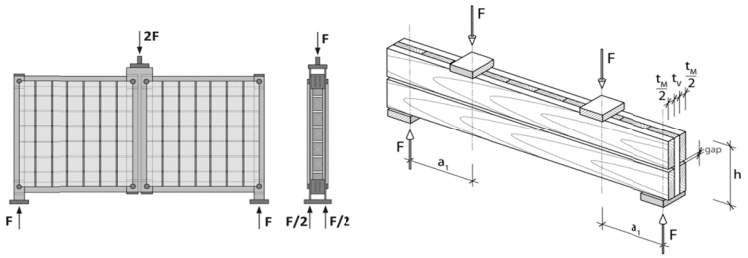

Fig. 3: Test configurations CLT elements: Traetta et al. (2006; left), CUAP (2006, right)

To summarise: until now test data regarding pure shear failures in CLT elements according to mechanism I are missing. The only reported single test, which failed in shear perpendicular to grain, is the one of Andreolli et al. (2012). Other investigations lead to failures others than in "net-shear". In fact, stress levels of τ_{net} at maximum test loads are in the range of 6.0 to 11.5 N/mm² on average. This indicates that the resistance of CLT against shear perpendicular to grain is even higher. Of course, the experiences made outline also the challenge in generating failures according to mechanism I in CLT elements.

In view of the motivation to establish bearing models, which base on strength and stiffness properties of the elements "boards" composing the system CLT, it is the aim to define reliable strength values for all three, in principle possible shear mechanisms. Based on them it is intended to provide bearing models, at least for representative CLT diaphragms, e.g. of 4 x 4 nodes, five layers and boards with w_l = 150 mm and t_l = 30 mm as reference.

2.2.2 Investigations on Nodes

Wallner (2004) investigated rolling shear strength and stiffness of nodes, in particular of the gluing interface, on three layer CLT of Norway spruce. The setup was a symmetrical three-point bending test with a loading in compression (see Fig. 4, left). Beside primary failures in rolling shear at the gluing interface, also shear failures parallel to grain in the horizontal board were observed. In that cases the mean shear stresses $\tau_{v,net,mean}$ at failures of several test series are in the range of 5.9 to 7.0 N/mm².

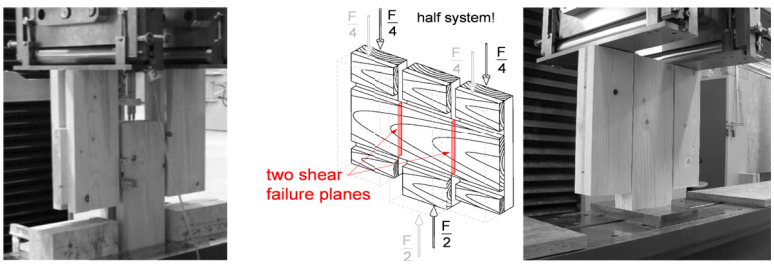

Fig. 4: Test configurations: Wallner (2004; left), Jöbstl et al. (2008; middle & right)

Based on Wallner (2004) and CUAP (2005) an adapted test configuration was developed for determining the bearing capacity of single nodes (Jöbstl et al. 2008; Fig. 4). The setup provides two possible failure planes of the cross section with w_l x t_l = 200 x 10 mm² at the vertical gaps with t_{gap} = 5 mm. As the weaker of both planes determines the ultimate load the test results are right censored. Jöbstl et al. (2008) did 20 tests with flat grain board material (Norway spruce) which all

successfully failed at the cross sections. The main statistics gained from tests are $f_{v,net,mean}$ = 12.8 N/mm², coefficient of variation $CV[f_{v,net}]$ = 11.3 % and the empirical 5 %-quantile $f_{v,net,05}$ = 11.1 N/mm². Applying maximum likelihood estimation (MLE) for right censored data, assuming a lognormal distribution with $f_{v,net} \sim$ 2pLND, the adapted statistics are $f_{v,net,mean,MLE}$ = 13.9 N/mm², $CV[f_{v,net,MLE}]$ = 13.5 % and $f_{v,net,05,MLE}$ = 11.0 N/mm².

In view of current design procedures, which verify the shear resistance on a single node (see Bogensperger et al. 2010) it is mandatory to define a test procedure for mechanism I which allows to quantify the relevant resistance reliable. In fact, interaction of mechanism I and II cannot be avoided. However, the interaction relationship has not been quantified until now. The test procedure has to allow for variation of test parameters in a range at least relevant for the practical use of CLT, e.g. in respect to the thickness and width of commonly used boards and the annual ring pattern, e.g. the differentiation between flat and rift grain boards. Based on a comprehensive comparison of current technical approvals of CLT available in Europe the common ranges in thickness t_l and width w_l of single lamellas are (12) 20 to 40 (45) mm and (40) 100 to 240 (300) mm, respectively (Brandner 2013).

3 Development and Verification of a Test Configuration

3.1 Principal Considerations

Based on the successfully proved test setup of Jöbstl et al. (2008) further developments were made in the frame of the Master thesis of Hirschmann (2011). Considering the test configuration for in plane shear strength of engineered wood products in EN 789 and the shear configuration for solid timber in EN 408 advancements of the setup of Jöbstl et al. (2008) were made, see Fig. 5. In brief: resultant forces of loading and support are in-line. The test specimen is rotated 14°, equal to the recommendations in EN 408. In contrast to the setup of Jöbstl et al. (2008) only one failure plane for shear loads perpendicular to grain is provided. This allows direct use of test results without further data processing, e.g. by means of MLE for right censored data. Another advantage is the possibility to gain the specimen directly from full-size CLT elements. A general disadvantage is the interaction of shear and compression perpendicular to grain in the cross layer. Consequently, the bearing capacity in shear is somehow overestimated. However, because of the small angle of 14° only a small influence is expected.

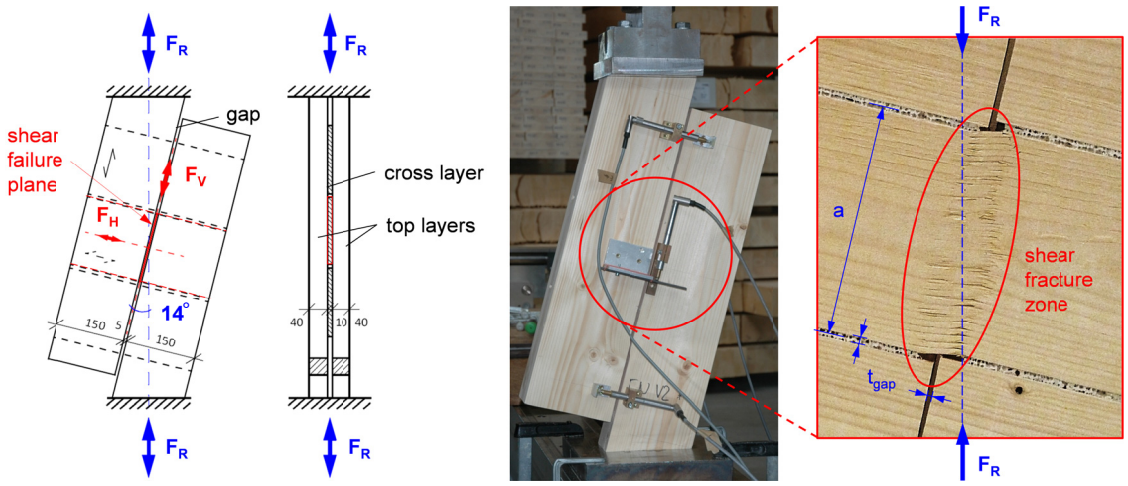

Fig. 5: Configuration and geometric parameters for testing shear perpendicular to grain on single CLT nodes by loading in tension or compression (left); test loaded in compression, including measurement of deformation and fractured cross section (right) (Hirschmann 2011; adapted)

Clarifying the possible influence of loading in tension or compression on the shear capacity two series of three specimen each were tested with core layers w_l x t_l = 150 x 10 mm². The mean shear strengths for loading in compression and tension are 9.6 N/mm² ($\rho_{12,mean}$ = 427 kg/m³) and 9.8 N/mm² ($\rho_{12,mean}$ = 423 kg/m³), respectively. The hypothesis of equal medians cannot be rejected (Mann-

Whitney test; $p = 0.7$). For convenience in test preparation and execution, the main series were tested in compression.

The aims of Hirschmann (2008) were (i) to investigate the applicability of the setup, (ii) to compare the results with that gained from the setup of Jöbstl et al. (2008), and (iii) to analyse the influences of selected geometric and material parameters on the shear perpendicular to grain resistance.

For clarification, the test series according to the setup of Jöbstl et al. (2008) are further given as "CIB" and that according to Hirschmann (2011) as "EN".

3.2 Material and Methods

The test material was Norway spruce (*Picea abies*) of nominal strength class C24 according to EN 408. All material was classified according to the density. Thus, "matched samples" for series "CIB" and "EN" were created. The material was conditioned at 20 °C and 65 % relative humidity to reach an expected average moisture content of $u = 12$ %. Ten tests per series were executed. In the reference test series "C" the core boards were flat grained (fgB) of w_l x $t_l = 150$ x 20 mm² and with gaps of $t_{gap} = 5$ mm. In all tests, top layers with 40 mm thickness were used. Following variations of parameters were made (see also Tab. 1):

- width w_l: 150, 200 mm;
- thickness t_l: 10, 20, 30 mm;
- annual ring orientation (AR): flat grain boards (fgB), rift grain boards (rgB) and heart boards (hB);
- gap width t_{gap}: 1.5, 5.0, 25.0 mm.

As no rift grain boards were available, "pseudo rift grain boards" were produced by trimming out the heart of heart boards and edge gluing of the residual parts.

The geometry of the test setups "CIB" and "EN" was planned to resist (i) compression at loading and support, (ii) torsion in the gluing interface, and (iii) rolling shear in the gluing interface until failing in shear perpendicular to grain in the net cross section of the core layer. A compilation can be found in Hirschmann (2011). The test segments in the core were taken consecutively from 4 m long boards with the aim to assure regions free of growth characteristics like knots, checks and reaction wood in the expected failure zone of the specimen. Consequently, in tested series one to five specimens are from the same board.

The tests were executed way controlled. The velocity was adapted to ensure an average time until ultimate load of 300 ± 120 s.

3.3 Test Results

A summary of tested parameters and of main statistics is provided in Tab. 1. All executed tests in series "CIB" and "EN" failed in the expected plane due to shear perpendicular to grain. Classification according to density was successful comparing the series with equal parameters of "CIB" and "EN". However, series "G", "H" and "I" of both setups show significant higher densities. For the test results of "CIB" a MLE for right censored data, as in chapter 2.2.2, was executed.

Although mean and median shear strengths at equal parameter settings in series "CIB" are always higher than in series "EN" (on average + 0.5 N/mm²), the hypothesis of equal medians cannot be rejected in five of seven paired groups (Mann-Whitney test, $p > 0.05$), beside of series "C" and "I". The reasons for systematically higher shear strengths in "CIB" are seen in the load path. Whereas setup "EN" provides resulting forces of loading and support in-line, in "CIB" the cross layer is additionally stressed in bending. Furthermore, it can be assumed that the load path in "CIB" in proportion to the shear stress leads to higher compression perpendicular to grain stresses. However, due to the moment also an interaction of tension perpendicular to grain and shear is given. Following the work of Spengler (1982) the higher compression stresses in "CIB" in comparison to "EN" are seen as reason for the roughly 5 % higher shear strengths in "CIB". A possible stiffening of the compression zone attracts additional loads. It is concluded that both configurations provide comparable test values. As the uncertainty in statistical inference in series "CIB" is higher and the load

path more complex, the test setup "EN" is preferred. Hirschmann (2011) also shows that in comparison to "CIB" the setup "EN" allows testing of a wider range in examined parameters.

Although the material quality and parameter settings are comparable, the mean and dispersion of $f_{v,net}$ in series "CIB_A" are significantly lower than in Jöbstl et al. (2008). In fact, in all series of Hirschmann (2011) an unexpected low coefficient of variation is observed. One reason is caused by the test preparation, whereby more than one specimen per series origin from the same board. Considering the hierarchical material structure of timber, in case of a second order hierarchical model with differentiation in variation within and between board properties, it is concluded that the results are somehow biased. As the assignment of test specimen to former boards is possible, estimates for coefficients of variation of $f_{v,net}$ within and between boards are 3.0 % and 3.6 %, respectively. Following Källsner et al. (1997) an equicorrelation coefficient, as measure for the correlation of $f_{v,net}$ within boards, can be estimated as $\rho_{equi} \approx 0.59$. This equicorrelation is higher than found on average for other strength properties (Brandner 2012). This is argued by the restriction of test material regarding growth characteristics and by a strict classification in density. The coefficient of variation of density $CV[\rho_{12}]$ is in the range of 2 % to 8 % (on average 4 %). However, the expected mean range is 6 % to 8 %; thus, the test material is very homogeneous. For material commonly used in timber engineering a higher variation in shear strength than the herein observed range in "EN" test series of $CV[f_{v,net}]$ = (5 to 10) % is expected. In view of the experiences reported in Jöbstl et al. (2008) a range of $CV[f_{v,net}]$ = (12 to 15) % and a lower equicorrelation appears reasonable.

Tab. 1: Test parameters and main statistics of density and shear strength at 12 % moisture content according to Hirschmann (2011); results partly adapted and reassessed

		EN								CIB						
		A	**B**	**C**	**D**	**F**	**G**	**H**	**I**	**A**	**B**	**C**	**F**	**G**	**H**	**I**
base p. [-]	**w_l [mm]**	**200**	**150**							**200**	**150**					
	t_l [mm]	**10**		**20**	**30**	**20**				**10**	**20**					
	AR [-] [1]	**fgB**				**rgB**	**hB**	**fgB**		**fgB**			**rgB**	**hB**	**fgB**	
	t_{gap} [mm]	**5.0**						**1.5**	**25.0**	**5.0**					**1.5**	**25.0**
ρ_{12} [kg/m³]	**quantity [-]**	à 10								à 10						
	mean	396	401	399	395	397	443	413	419	405	400	397	398	435	424	439
	median	396	404	400	400	395	444	413	416	405	396	407	397	432	427	453
	CV [%]	1.8	4.4	2.6	3.7	3.3	1.9	8.4	7.0	3.0	4.2	5.6	6.9	2.4	1.8	7.0
$f_{v,net,12}$ [N/mm²]	**min**	10.0	10.2	8.4	6.4	6.3	8.2	8.5	7.1	–	–	–	–	–	–	–
	mean	**10.8**	**11.2**	**8.9**	**7.5**	**7.2**	**8.8**	**9.5**	**8.0**	**11.1** [2]	**11.7** [2]	**9.4** [2]	**8.0** [2]	**9.2** [2]	**9.8** [2]	**8.8** [2]
	median	**10.8**	**11.2**	**8.7**	**7.4**	**7.4**	**8.9**	**9.3**	**8.1**	**11.0** [2]	**11.7** [2]	**9.4** [2]	**7.9** [2]	**9.2** [2]	**9.8** [2]	**8.7** [2]
	max	12.1	12.4	9.6	8.4	8.0	9.4	10.6	8.6	–	–	–	–	–	–	–
	CV [%]	6.0	6.3	4.9	9.3	10.1	4.2	8.5	5.6	7.4 [2]	6.9 [2]	7.4 [2]	15.1 [2]	7.4 [2]	5.2 [2]	7.9 [2]
	5 %-qu.	10.1 [3]	10.3 [3]	8.5 [3]	6.7 [3]	6.3 [3]	8.3 [3]	8.5 [3]	7.2 [3]	9.8 [2]	10.4 [2]	8.3 [2]	6.2 [2]	8.2 [2]	9.0 [2]	7.7 [2]

[1] AR … annual ring orientation | fgB … flat grain boards | rgB … "pseudo" rift grain boards | hB … heart boards

[2] statistics estimated by means of Maximum Likelihood Estimation (MLE) for right censored data, assuming $f_{v,net} \sim$ 2pLND

[3] empirical 5 %-quantile, gained from rank statistics

3.4 Shear Perpendicular to Grain: Load-Displacement and Failure Behaviour

Both setups, "EN" and "CIB", show similar characteristic load-displacement behaviour, see Fig. 6 (left). The load-displacement curve can be divided in two main parts: the first part showing a roughly linear course until the ultimate load F_{max} is reached, and the second part a clear softening property, where failure due to a new shear mechanism can be observed (see also Fig. 5, right).

In the first part, after some hardening until approximately 20 % of F_{max}, a linear elastic material behaviour within approximately $0.2 \cdot F_{max}$ to $0.8 \cdot F_{max}$ is given, followed by a regressive non-linear relationship until F_{max}. At this point, a combined failure of shear mechanisms I "net-shear" and II "torsion" takes place, initiated by local exceeded resistance in opposite corners of the failure plane, at the zones of interacting shear and tension perpendicular to grain. In the second part after the peak load, softening is characterised by reaching a steady state at about 40 % to 50 % of F_{max}, enabling large

deformations. These deformations increase shearing parallel to grain, mainly in the transition zone of early- and latewood. It follows a successive dissolution of the material by separation of annual rings. This leads to a flexible composite of fixed-end beams, active in bending and tension parallel to grain (see also Jöbstl et al. 2008).

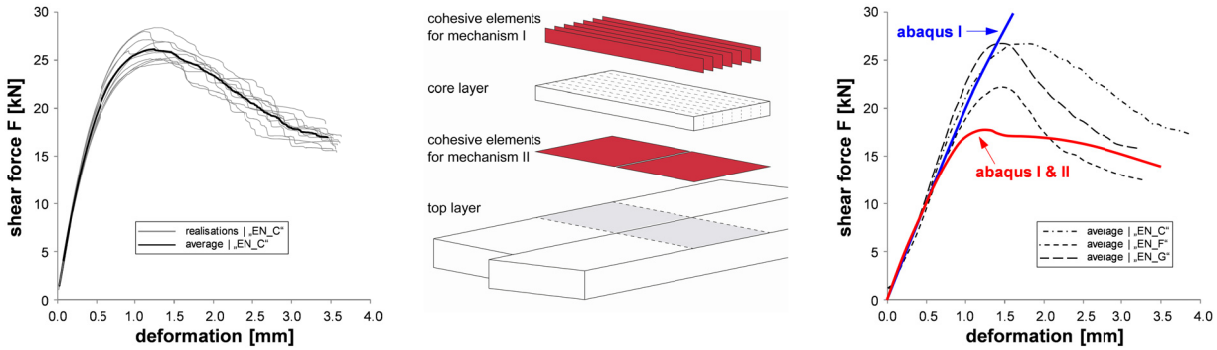

Fig. 6: Typical load-displacement behavior exemplarily for series "EN_C": single and average curves (left); placement of cohesive elements in the numerical model (middle); comparison of average load-displacement curves with the numerical results on characteristic (5 %-quantile) level (right)

The complexity of the failure behaviour motivated a numerical model with the aim to mirror the load-displacement curve in a satisfying manner. Therefore, a FE-model with cohesive elements was implemented in ABAQUS. These elements allow fracturing in the observed failure planes by following the Dugdale-Barenblatt model of elastic-plastic fracture mechanics. Separation in fracture mode I and shear sliding in mode II and III according to this theory occur after a critical stress value has been achieved. Thus, characteristic (5 %-quantile) strength values and fracture energies are input parameters of the numerical model, see Feichter (2013).

To account for both shear mechanisms, mechanism I "net-shear" and II "torsion", cohesive elements must be implemented in both failure regions, see Fig. 6 (middle). The outcome of the numerical model is shown in Fig. 6 (right) together with the average load-displacement curves from series "EN_C" (fgB), "EN_G" (hB) and "EN_F" (rgB). Numerical results are shown for (i) cohesive elements only for mechanism I (abaqus I), and (ii) cohesive elements for mechanism I and II (abaqus I & II). The annual ring orientation was not considered in the numerical model. However, the results of the numerical study clearly outline, that at F_{max} both mechanisms, I and II, take place and consequence also the non-linear load-displacement behaviour before F_{max}, and the softening afterwards.

The sequence in the fracturing process can also be explained by means of a simple engineering model, see Fig. 7. Thereby and under the circumstance of a supposed lateral support by orthogonal boards, a simple planar model of slender fixed-end beams is considered in the shear area. For simplicity, this fixed-end beam is replaced by a fixed cantilever beam with half in length from left support to the middle, where an asymmetric boundary condition acts and shear force can be introduced. Following assumptions are made:

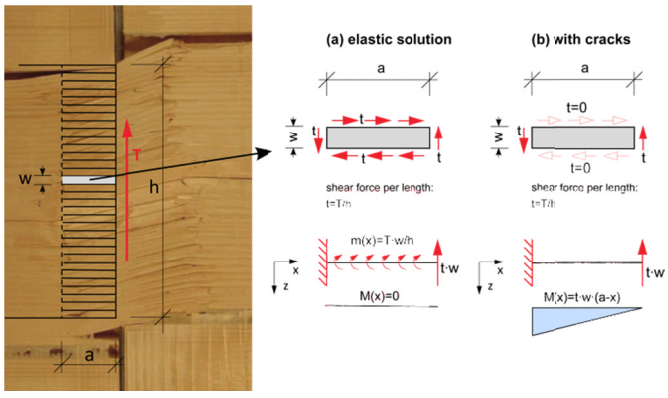

Fig. 7: Simple engineering model

- T is the total shear force to be transmitted;
- the elastic behaviour dominates at beginning (a); after fracture the loading changes to (b).

It can be easily shown that the elastic solution (a) transmits shear forces as a pure shear field without bending. After cracking shear forces can only be transferred via the cross sections of the cantilever (b). In that case a linear increasing bending moment develops and consequences a successive failure of the cantilever in bending and tension.

In brief: failure at F_{max} due to shear forces perpendicular to grain is caused by exceeding the local resistance of interacting mechanism I and II. The numerical model verifies this. Further a softening to a steady state at approximately 40 % to 50 % of F_{max} is given. A successive dissolution of the shear fracture zone, by increasing shearing parallel to grain at the transition zone of early- and latewood and separation of the annual rings, occurs. A flexible composite of fixed-end beams becomes active in tension and bending. This is the cause for the high residual forces. A simple engineering model demonstrated this sequence of fracturing. However, there is no doubt that the shear forces applied perpendicular to grain lead to shearing parallel to grain. Consequently, the shear capacities and the shear behaviour parallel to grain, in reference to a relatively small shear area and volume, indicate the shear resistance perpendicular to grain.

3.5 Main influencing Parameters

In the following the investigated parameters (i) annual ring orientation, (ii) layer width, (iii) layer thickness, and (iv) gap width are discussed individually regarding a possible influence on the shear capacity perpendicular to grain. For statistical inference the Mann-Whitney test was used for testing the hypothesis of pairwise equal medians. This was done although a symmetric distribution is not realised in all series. Box-plots of all results of setup "EN" together with median values of setup "CIB" are provided in Fig. 8.

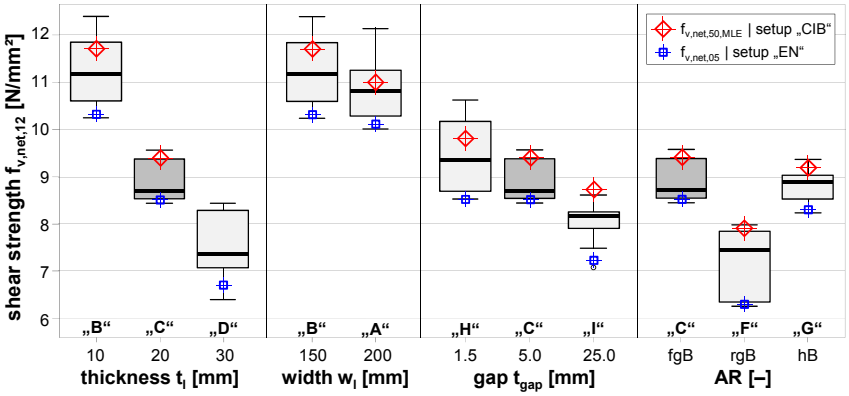

Fig. 8: Box-plot of shear strength $f_{v,net,12}$ of setup "EN" vs. parameter variations; median values of setup "CIB" included

3.5.1 Annual Ring Orientation

Investigating the influence of AR, the following series were tested: series "C" comprising flat grain boards (fgB), series "F" with "pseudo" rift grain boards (rgB) and series "G" with heart boards (hB). The parameters width $w_l = 150$ mm, thickness $t_l = 20$ mm and gap width $t_{gap} = 5$ mm were kept constant. The average densities of "fgb" and "rgB" are well comparable whereas both series "EN_G" and "CIB_G" (hB) show significantly higher densities (mean difference 30 to 40 kg/m³). The results are presented in Fig. 8.

As shear loads perpendicular to grain lead to failures in shear parallel to grain (see chapter 3.4) there is evidence for influences caused by the parameter "annual ring orientation". Keenan et al. (1985), Denzler and Glos (2007), Dahl and Malo (2009) and Brandner et al. (2012) found significant higher shear strength (on average 6 % to 40 %) in RL (radial-longitudinal) in comparison to TL direction (tangential-longitudinal), Müller et al. (2004) not. In TL shearing occurs in the transition zone of early- und latewood. In RL, shearing requires fracturing of early- and latewood. Consequently, a higher resistance and a positive dependency of $f_{v,RL}$ on specimen's global density are expected. Thus, flat grain boards, in comparison to rift grain and heart boards, have commonly a higher resistance in shear. The annual ring orientation in heart boards may comprise both, shearing in RL in the core and in TL at the edges. In dependency of the width of the core lamella a resistance in-between flat and rift grain boards is expected.

Statistical inference confirms the expectations regarding significant lower shear strengths in rift grain boards in comparison to flat grain boards ($p < 0.01$). Also between series "rgB" and "hB" significant differences in the medians are observed ($p < 0.01$). Some impact of the significant higher density in

series “hB” cannot be excluded. As flat grain boards are commonly used in CLT production, relatively high shear resistances can be realised. However, in both setups, “EN” and “CIB”, an interaction of shear and compression perpendicular to grain occurs. Keenan (1973, 1974) observed that $f_{v,RL}$ is much more influenced in case of interaction with $\sigma_{c,90}$ than $f_{v,TL}$.

3.5.2 Layer Width

A comparison is made between $w_l = 150$ mm (series “A”) and 200 mm (series “B”) wide boards. This corresponds to a ratio of 1 : 1.33. The parameters $t_l = 10$ mm, $t_{gap} = 5$ mm and AR = “fgB” were kept constant. The average densities of all series are in-line. Comparison shows that the hypothesis of equal medians cannot be rejected ($p > 0.05$). This is also obvious considering the comparable ranges of realisations in series “A” and “B”, see Fig. 8. However, as the range in commonly used board widths ($100 \text{ mm} \leq w_l \leq 240$ mm) is much larger than tested some relevant influence on the shear resistance cannot be excluded, in particular in wide boards were shearing at the edges more and more occurs in TL, known to realise lower shear resistances (see chapter 3.5.1).

3.5.3 Layer Thickness

Test series “B” ($t_l = 10$ mm), “C” ($t_l = 20$ mm) and “D” ($t_l = 30$ mm) were conducted for examining the influence of layer thickness. The parameters $w_l = 150$ mm, $t_{gap} = 5$ mm and AR = “fgB” were kept constant. The average densities of all series are in-line. The results are visualised in Fig. 8. In both test setups “EN” and “CIB” and in all pairwise comparisons the hypothesis of equal medians was rejected ($p < 0.01$). Two main reasons are identified: at first, the impact of size on shear strength parallel to grain is well known and documented, e.g. in Brandner et al. (2012). They report on a regressive course of shear strength with increasing shear area A_s. Secondly, load transfer from top layers to the core layer via the gluing interfaces causes a locking effect. This locking effect, which restrains the shear action, is at highest in the gluing interface and declines until the centre of the core lamella.

Fig. 9 contains a comparison of the size effect on shear strength parallel to grain for construction timber, based on a literature survey and tests reported in Brandner et al. (2012), some additional data sets for clear wood and the results found for setup “EN”. The plot shows the shear strength versus the shear area A_s. Deviating from the definition of A_s in Brandner et al. (2012), for the herein presented test setup and results A_s is defined by the cross section of the core lamella, with $A_s = w_l \cdot t_l$. Overall, good congruence is found. The steeper regressive course in $f_{v,net,mean}$ vs. the shear area A_s is dedicated to the locking effect. In view of the tendency to standard lamella thicknesses $t_l = 20$, 30, 40 mm an extrapolation for 40 mm thick lamellas is required.

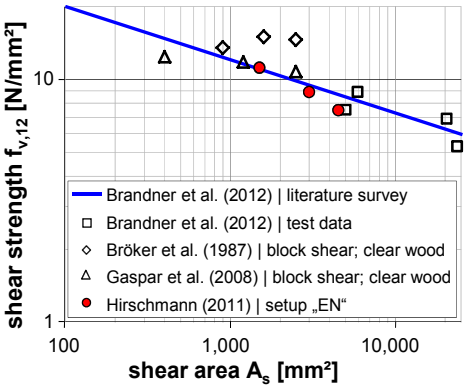

Fig. 9: Size effect on mean shear strength

3.5.4 Gap Width

The influence of gap width on shear strength was analysed for $t_{gap} = 1.5$ mm (series “H”), 5.0 mm (series “C”) and 25.0 mm (series “I”). The parameters $w_l = 150$ mm, $t_l = 20$ mm and AR = “fgB” were kept constant. The average densities of series “H” and “I” are well comparable whereas both series “EN_C” and “CIB_C” ($t_{gap} = 5.0$ mm) show significantly lower densities (mean differences of 15 to 20 kg/m³ in “EN” and 25 to 40 kg/m³ in “CIB”). Because of the dependency of $f_{v,RL}$ on the density in softwood, an influence on $f_{v,net}$ cannot be excluded. The results are shown in Fig. 8.

As a quantitative correction of the differences in density is not available statistical inference is made on observed pairwise median shear strengths. Significant differences in medians are found between $t_{gap} = 1.5$ mm and 5.0 mm and 5.0 mm and 25.0 mm in setup “CIB” ($p < 0.05$). High significant differences ($p < 0.01$) are identified between $t_{gap} = 1.5$ mm and 25.0 mm in both setups “EN” and “CIB” and between $t_{gap} = 5.0$ mm and 25.0 mm in “EN”. However, the hypothesis of equal medians cannot be rejected comparing series with $t_{gap} = 1.5$ mm and 5.0 mm in setup “EN” ($p = 0.10$).

In general, a decrease in the resistance with increasing gap width is expected. This is because of a reduced influence of the locking effect as well as by increasing bending stresses in the gap. Thus, a regressive course of shear strength versus gap width is expected.

4 Resistance in Shear Loads perpendicular to Grain: Proposal

In chapter 3 the resistance against shear loads perpendicular to grain was demonstrated and relevant influencing parameters identified. The interaction of shear and compression perpendicular to grain, which leads to some overestimation of the real shear resistance, was mentioned. However, at the ultimate load interaction of shear mechanisms I "net-shear" and II "torsion" may counteract the shear-compression interaction. In view of the material commonly used for CLT in Europe, flat grain boards with cross section w_l x t_l = 150 x 30 mm² and a gap width of t_{gap} = 5 mm (as upper boundary) are defined as reference. Furthermore, a lognormal distribution ($f_{v,net}$ ~ 2pLND) and a coefficient of variation $CV[f_{v,net}]$ = 15 % are assumed. Based on $f_{v,net,12,mean}$ = 7.5 N/mm² in series "EN_D" the characteristic (5 %-quantile) shear strength is $f_{v,net,05}$ = 5.8 N/mm². In case of lamellas with t_l = 40 mm, as the upper boundary of commonly used raw material, a value of $f_{v,net,05}$ = 5.3 N/mm² is found by extrapolating the power regression model, based on mean values of series "EN_B", "EN_C" and "EN_D". However, these strength values are gained from examinations made on single nodes of a three layer CLT element. The question remains if the verification of shear in plane, currently done on single nodes and RVSEs, is representative for a whole CLT diaphragm. As demonstrated in chapter 2 this question cannot be answered yet, but an engineering judgement can be made.

In view of the bearing model for CLT in bending out of plane, we define a reference CLT diaphragm of 4 x 4 nodes and of five layers, each composed of board material in reference dimension. Assuming a shear load, homogeneously applied on the cross sections of this diaphragm, in total two times the tested node in thickness direction are found to act in parallel. Due to allocated shear stresses, a failure of the diaphragm in plane according to "net-shear" can only take place in cases where all nodes in *x*-direction (direction of the top layers) fail. Again, a parallel system action, active in *y*-direction (direction of the cross layers) of the diaphragm, can be identified. Of course, in a 4 x 4 element this kind of shearing can occur on three planes, whereby the weakest plane governs the ultimate load. This confirms to a serial system action, active in *x*-direction of the diaphragm. Considering the load-displacement curve of shear perpendicular to grain, a non-linear behaviour, already before reaching the ultimate load, and the ability to withstand large deformations on a moderate load level after softening is found. Taking into account the remarkable possibility to transfer loads between the parallel active nodes, there is evidence that the mean resistance of the diaphragm in shear will not be remarkable different from the mean shear resistance of single nodes. However, because of the parallel system action of 2 x 4 nodes a significant reduction in dispersion of $f_{v,net}$ is expected. On the one hand this circumstance reduces the influence of serial system action between the shear planes, and on the other hand it offers the possibility of rising $f_{v,net,05}$.

Although a theoretical and practical verification is not available yet the current procedure of verifying in plane shear resistance on single nodes (see e.g. Bogensperger et al. 2010) is judged as reliable and proposed in the meantime until further progress is made. For simplicity a characteristic (5 %-quantile) shear strength of $\boldsymbol{f_{v,net}}$ **= 5.5 N/mm²** is proposed for all lamella thicknesses $t_l \leq 40$ mm.

5 Conclusions and Outlook

We presented a test configuration, which allows determining the resistance in shear perpendicular to grain on single CLT nodes. Relevant parameters were investigated and their influence on shear strength $f_{v,net}$ quantified. Thereby, the parameters (i) thickness of the core lamella t_l, (ii) the annual ring orientation *AR*, and (iii) the gap width t_{gap} were found to affect the shear strength significantly.

Additional to testing, the load-displacement behaviour and in particular the failure process were studied by means of a numerical and a simple engineering model. The interaction of both shear mechanisms, mechanism I "net-shear" and II "torsion", the fracturing in shear parallel to grain and

successive dissolution of the material was verified. Analogies to shear resistance parallel to grain of structural timber were identified, in particular regarding the size effect.

Based on engineering judgement the shear resistance according to mechanism I was discussed for a whole CLT diaphragm. In conclusion, a characteristic (5 %-quantile) value of $f_{v,net,05}$ = 5.5 N/mm² for common flat grain board material of Norway spruce with $t_l \leq 40$ mm and $t_{gap} \leq 5$ mm, and the verification of shear in plane on single nodes or RVSEs, including both, the verification of mechanism I and II, is proposed.

Current investigations are made on a hardening property after softening and on the shear resistance at $t_{gap} = 0$. Fig. 10 illustrates first results of flat and rift grain boards at $t_{gap} = 5$ and 0 mm. Although and not to the full extend relevant for the shear behaviour of a whole CLT diaphragm, a tremendous ability to large deformations at a steady state on a relatively high load level, followed by a hardening which exceeds mostly the first, currently evaluated peak level, is observed. Further tests and investigations on whole CLT elements are scheduled.

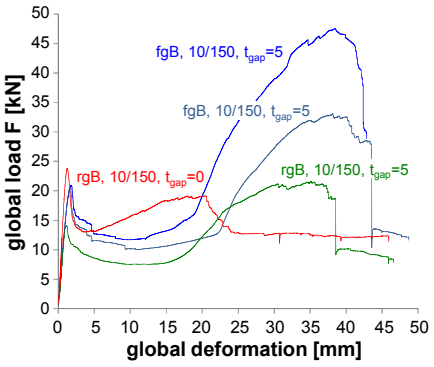

Fig. 10: Single test results on specific parameter settings

6 Acknowledgement

The work and progress made by Hirschmann (2011) and Feichter (2013), as part of their Master theses, is thankfully acknowledged. Thanks also to Prof. Roberto Tomasi from University of Trento / Italy for discussing several aspects concerning the tests published in Andreolli et al. (2012).

7 References

Andreolli M, Tomasi R, Polastri A (2012) **Experimental investigation on in-plane behaviour of cross-laminated-timber elements**. Paper and Presentation, CIB-W18/45-12-4, Växjö, Sweden

Blaß H J, Görlacher R (2002) **Zum Trag- und Verformungsverhalten von Brettsperrholz-Elementen bei Beanspruchung in Plattenebene**. *Bauen mit Holz*, 11:34–41; 12:30–34 (in German)

Blaß H J, Flaig M (2012) **Stabförmige Bauteile aus Brettsperrholz**. Karlsruher Berichte zum Ingenieurholzbau, No. 24, Karslruher Institut für Technologie (KIT), Lehrstuhl für Ingenieurholzbau und Baukonstruktionen, ISBN 978-3-86644-922-0 (in German)

Bogensperger T, Moosbrugger T, Schickhofer G (2007) **New test configuration for CLT-wall-elements under shear load**. CIB-W18/40-21-2, Bled, Slovenia

Bogensperger T, Moosbrugger T, Silly G (2010) **Verification of CLT-plates under loads in plane**. WCTE'2010, Riva del Garda, Italy

Bosl R (2002) **Zum Nachweis des Trag- und Verformungsverhaltens von Wandscheiben aus Brettlagenholz**. Dissertation, Universität der Bundeswehr München, Fakultät für Bauingenieur- und Vermessungswesen (in German)

Brandner R (2012) **Stochastic system actions and effects in engineered timber products and structures**. Dissertation, Institute of Timber Engineering and Wood Technology, Graz University of Technology

Brandner R, Gatternig W, Schickhofer G (2012) **Determination of Shear Strength of Structural and Glued Laminated Timber**. CIB-W18/45-12-2, Växjö, Sweden

Brandner R (2013) **Production and Technology of Cross Laminated Timber (CLT): A state-of-the-art Report**. In: Harris R, Ringhofer A, Schickhofer (ed.) Focus Solid Timber Solutions – European Conference on Cross Laminated Timber (CLT), 21st–22nd May 2013, Graz, Austria

Bröker F W, Meierhofer U A, Radović B (1987) **Einfluss der Probengröße auf die Druckscherfestigkeiten würfelförmiger Fichtenholzproben**. *Holz als Roh- und Werkstoff*, 45:445–448 (in German)

CUAP Common Understanding of Assessment Procedure (2005) **Solid wood slab element to be used as a structural element in buildings**. ETA request No 03.04/06, Österreichisches Institut für Bautechnik (OIB), Vienna, Austria

Dahl K B, Malo K A (2009) **Linear shear properties of spruce softwood**. *Wood Science and Technology*, 43:499–525

Denzler J K, Glos P (2007) **Determination of shear strength values according to EN 408**. *Materials and Structures*, 40:79–86

EN 338:2009-10 **Structural timber – Strength classes**. European Standard, European Committee for standardization

EN 408:2012-07 **Timber structures – Structural timber and glued laminated timber – Determination of some physical and mechanical properties**. European Standard, European Committee for standardization

EN 789:2004-10 **Timber structures – Test methods – Determination of mechanical properties of wood based panels**. European Standard, European Committee for standardization

Feichter I (2013) **Spannungs- und Traglastberechnungen an ausgewählten Problemen der Holz-Massivbauweise in Brettsperrholz**. Master thesis, Institute of Timber Engineering and Wood Technology, Graz University of Technology (in German)

Flaig M, Blaß H J (2013) **Shear strength and shear stiffness of CLT-beams loaded in plane**. CIB-W18/46-12-3, Vancouver, Canada

Gaspar F, Cruz H, Gomes A (2008) **Evaluation of glued laminated timber structures – core extraction and shear testing**. World Conference on Timber Engineering (10th WCTE), Miyazaki, Japan

Hirschmann B (2011) **Ein Beitrag zur Bestimmung der Scheibenschubfestigkeit von Brettsperrholz**. Master thesis, Institute of Timber Engineering and Wood Technology, Graz University of Technology (in German)

Jeitler G (2004) **Versuchstechnische Ermittlung der Verdrehungskenngrößen von orthogonal verklebten Brettlamellen**. Diploma thesis, Institute of Steel, Timber and Shell Structures, Graz University of Technology (in German)

Jöbstl R A, Bogensperger T, Schickhofer G, Jeitler G (2004) **Mechanical Behaviour of Two Orthogonally Glued Boards**. WCTE'2004, Lahti, Finland

Jöbstl R A, Bogensperger T, Schickhofer G (2008) **In-plane shear strength of cross laminated timber**. CIB-W18/41-12-3, St. Andrews, Canada

Källsner B, Ditlevsen O, Salmela K (1997) **Experimental verification of a weak zone model for timber in bending**. IUFRO S 5.02 – Timber Engineering, Copenhagen, Denmark

Keenan F J (1973) **The shear strength of glued-laminated timber**. University of Toronto, Department of Civil Engineering

Keenan F J (1974) **Shear strength of wood beams**. *Forest Products Journal*, 24(9):63–70

Keenan F J, Kryla J, Kykong B (1985) **Shear strength of spruce glued-laminated timber beams**. *Canadian Journal of Civil Engineering*, 12:661–672

Kreuzinger H, Sieder M (2013) **Einfaches Prüfverfahren zur Bewertung der Schubfestigkeit von Kreuzlagenholz / Brettsperrholz**. *Bautechnik*, 90(5):314–316 (in German)

Müller K, Sretenovic A, Gindl W, Grabner M, Wimmer R, Teischinger A (2004) **Effects on macro- and micro-structural variability on the shear behaviour of softwood**. *IAWA Journal*, 25(2):231–243

Spengler R (1982) **Festigkeitsverhalten von Brettschichtholz unter zweiachsiger Beanspruchung, Teil 1 – Ermittlung des Festigkeitsverhaltens von Brettelementen aus Fichte durch Versuche**. Berichte zur Zuverlässigkeitstheorie der Bauwerke, Heft 62, Laboratorium für den konstruktiven Ingenieurbau, Technische Universität München (in German)

Traetta G, Bogensperger T, Moosbrugger T, Schickhofer G (2006) **Verformungsverhalten von Brettsperrholzplatten unter Schubbeanspruchung in der Ebene**. In: Moosbrugger M, Schickhofer G, Unterwieser H, Krenn H (ed.) Brettsperrholz – Ein Blick auf Forschung und Entwicklung. 5. Grazer Holzbau-Fachtagung (5.GraHFT'06), 29th Sept. 2006, Graz, Austria (in German)

Wallner G (2004) **Versuchstechnische Ermittlung der Verschiebungskenngrößen von orthogonal verklebten Brettlamellen**. Diploma thesis, Institute of Steel, Timber and Shell Structures, Graz University of Technology (in German)